Electronic excitations in 3*d* transition metals

P. Unger
Max-Planck-Institut für Physik komplexer Systeme, Außenstelle Stuttgart, 70569 Stuttgart, Germany

J. Igarashi
Faculty of Engineering, Gunma University, Kiryu, Gunma 376, Japan

P. Fulde
Max-Planck-Institut für Physik komplexer Systeme, 01187 Dresden, Germany
(Received 24 May 1994)

We calculate the direct and inverse photoemission spectra of 3*d* transition metals with fcc or bcc structure. The dynamics of the *d* electrons is described by an extended Hubbard model including five canonical *d* bands in the one-particle operator H_0 and all relevant on-site Coulomb and exchange matrix elements in the interaction Hamiltonian H_1. For the ground state a quantum-chemical ansatz is made taking local spin and density correlations into account. The retarded Green's functions of the *d* electrons are evaluated by using the projection technique of Mori and Zwanzig. Thereby the dynamics of the additional particle is projected onto local spin and density excitations in analogy to the ground-state calculation and treated exactly within that restricted operator space. In the case of Ni the correct satellite position and a reasonable reduction factor of the bandwidth are obtained by using an experimentally determined parameter set. The numerical calculations for our model Hamiltonian also predict multiplet structures in the photoemission spectra of Co and Fe.

I. INTRODUCTION

Transition metals provide a good example for a class of materials in which electronic correlations considerably influence the excitation spectrum as well as ground-state properties. When comparing angle-resolved photoemission data to band-structure calculations based on the local density approximation (LDA) a clear reduction of the *d* bandwidth due to correlations is observed. The experimental width turns out to be smaller by 10% for Fe and at least 25% for Ni.[1–3] Furthermore, measurements on Ni reveal an additional satellite structure 6 eV below the Fermi edge,[4,5] a feature impossible to explain within an independent-particle picture.

An important correlation effect is the screening of a test charge by the surrounding electrons. Due to this phenomenon the long-ranged Coulomb forces between electrons in metals are reduced to a screened interaction which decreases rapidly with distance. Inclusion of the screening of the Coulomb interaction is the basic idea of the GW approximation in which the usual Fock diagram is replaced by a screened exchange process. By applying this technique Aryasetiawan[6] was able to describe accurately the band narrowing and the broadening of the quasiparticle peaks in ferromagnetic Ni. However, the satellite structure at 6 eV could not be reproduced.

Most of the theoretical work on one-particle excitations in transition metals is based on (extended) Hubbard models.[7] In addition to the one-particle Hamiltonian H_0, which contains the (five) tight-binding bands of the *d* electrons near the Fermi energy, one considers the two-particle operator H_1 describing local Coulomb and exchange interactions within single transition-metal ions. The validity of this model Hamiltonian relies on the short-ranged nature of the screened Coulomb interaction and on the good localization of the *d* orbitals in transition metals (narrow band systems).

The simplest way of including correlation effects in the Hubbard model is by calculating self-energy corrections in second-order perturbation theory. Along this line Treglia *et al.*[8] obtained band narrowing as well as satellite structures. However, for a quantitative comparison with experiments higher-order corrections have to be included. The correlation energy of the ground state, for example, is overestimated by a factor of $2-3$ if one considers only processes up to second order.

In the *t*-matrix approach of Kanamori[9] the multiple scattering of two holes is taken into account up to infinite order. However, the theory is restricted to the limit of low charge-carrier concentrations where it finally becomes exact. It has first been used by Penn[10] and Liebsch[11] to explain the appearance of a satellite structure in Ni. Later Liebsch[12] and Igarashi[13,14] went beyond the low-density limit by considering also multiple electron-hole scattering processes. The electron-hole scattering channel is closely related to the dynamic susceptibility, containing also contributions from the magnon poles when the system is magnetic. Consequently, their results may be compared with calculations based on magnon-hole coupling, which were performed independently by Roth,[15] Hertz and Edwards,[16] and Matsumoto *et al.*[17] Finally, band narrowing and a satellite structure for Ni have also been derived by Davis and Feldkamp,[18] who assumed the 3*d* self-energy to be the same as that of a core hole.

Besides these analytical calculations there exist also

0163-1829/94/50(15)/10485(13)/$06.00

numerical approaches to the correlation problem in a five-band Hubbard model: Victora and Falicov[19] calculated the exact single-particle spectrum for a four-center tetrahedral cluster with five d orbitals per site. By applying periodic boundary conditions the cluster simulates a four-atom fcc crystal. In this exact diagonalization study a correctly positioned multiplet structure and reasonable values for the band narrowing have been obtained for ferromagnetic Ni. But the details of the quasiparticle dispersion are beyond the scope of this cluster calculation which is restricted to the Γ and X points of the fcc Brillouin zone.

Local correlations of d electrons in transition metals can also be described using an Anderson impurity model as starting point. Thereby one considers a single transition-metal ion coupled to a sea of conduction electrons. Following this line Jo *et al.*[20] gave detailed interpretations of the $3d$ photoemission spectrum of ferromagnetic Ni and its resonant behavior at the $2p$ threshold. As in the cluster diagonalization mentioned before the quasiparticle dispersion cannot be obtained within that framework.

The treatment of one-particle excitations in transition metals presented here uses a quantum-chemical approach to the correlation problem. For the ground state an ansatz is made which includes local density and spin correlations. This part of our calculation is based upon the work of Stollhoff, Thalmeier, and Olés on transition metals, who applied the local ansatz to determine the properties of a ground state with paramagnetic[21] or ferromagnetic[22] spin order. It was found that electronic correlations within d orbitals lead to a considerable decrease of charge fluctuations and a buildup of local moments reflecting Hund's rules. For simplicity, a paramagnetic ground state is assumed in this work. Recently the local ansatz has been combined with the Monte Carlo technique by Takahashi and Kanamori[23] to investigate the ground state of Ni compounds.

In the framework of the local ansatz an accurate treatment of correlations in excited states is also possible. This has been demonstrated for semiconductors in Refs. 24 and 25 where sizable correlation corrections to the energy gaps of Si, Ge, and diamond were calculated. Later the treatment of quasiparticle energies was extended by Becker, Brenig, and Fulde[26] to a complete determination of the excitation spectrum. Thereby a formulation of the correlation problem in the framework of the projection technique of Mori[27] and Zwanzig[28] turned out to be very useful.

The projection technique is also applied in the present work for evaluating the retarded Green's functions of d electrons. Thereby we project the dynamics onto operators which generate the additional particle accompanied by local density or spin excitations. An essential point is the evaluation of matrix elements in coordinate space, which enables us to consider the three-particle scattering problem up to infinite order as in the t-matrix approach. Furthermore, the interaction operator H_1 may be taken to be quite general.

The paper is organized as follows. In Sec. II the model Hamiltonian is introduced. The ansatz for the correlated ground state is discussed in Sec. III. The correlation operators for the excited states correspond directly to this ansatz, as shown in Sec. IV. The numerical results for the ground state are briefly discussed in Sec. V. Subsequently we present the excitation spectra of Ni in Sec. VI and of the remaining $3d$ transition metals in Sec. VII. Details of the calculation are explained in the Appendixes.

II. THE MODEL

The calculation is based on a model Hamiltonian H describing a cubic lattice (fcc or bcc) with five d orbitals at each site. The one-particle term H_0' contains a summation over five canonical d bands $m = 1, ..., 5$ with dispersion relations $\epsilon_{m\mathbf{k}}$. The tight-binding band structure depends solely on the crystal structure and the total d bandwidth W (for details see Refs. 29 and 30). Therefore, canonical bands are well suited for a systematic treatment of different transition metals. The effect of hybridization between d and s electrons will be taken into account by assuming a noninteger occupation number n_d for d electrons. If we neglect the Coulomb interaction V between orbitals on different lattice sites I the Hamilton operators H_0' and H_1' can be written in the general form

$$H_0' = \sum_{m\mathbf{k}\sigma} \epsilon_{m\mathbf{k}} d^\dagger_{m\mathbf{k}\sigma} d_{m\mathbf{k}\sigma}, \tag{1}$$

$$H_1' = \frac{1}{2} \sum_{I\sigma\sigma'} \sum_{ijkl} V_{ijkl}\, d^\dagger_{iI\sigma} d^\dagger_{kI\sigma'} d_{lI\sigma'} d_{jI\sigma}. \tag{2}$$

Here, the operator $d^\dagger_{m\mathbf{k}\sigma}$ creates a d electron with wave vector $\mathbf{k}$ in band m with spin σ. It is related to the local creation operators $d^\dagger_{iI\sigma}$ through

$$d^\dagger_{m\mathbf{k}\sigma} = N^{-\frac{1}{2}} \sum_{iI} e^{-i\mathbf{k}\cdot\mathbf{R}_I} \gamma_{mi}(\mathbf{k})\, d^\dagger_{iI\sigma}. \tag{3}$$

TABLE I. Matrix of exchange constants J_{ij} for the five different d orbitals.

	zx	yz	xy	x^2-y^2	$3z^2-r^2$
zx	0	$J-\frac{1}{2}\Delta J$	$J-\frac{1}{2}\Delta J$	$J-\frac{1}{2}\Delta J$	$J-\frac{5}{2}\Delta J$
yz	$J-\frac{1}{2}\Delta J$	0	$J-\frac{1}{2}\Delta J$	$J-\frac{1}{2}\Delta J$	$J-\frac{5}{2}\Delta J$
xy	$J-\frac{1}{2}\Delta J$	$J-\frac{1}{2}\Delta J$	0	$J-\frac{7}{2}\Delta J$	$J+\frac{1}{2}\Delta J$
x^2-y^2	$J-\frac{1}{2}\Delta J$	$J-\frac{1}{2}\Delta J$	$J-\frac{7}{2}\Delta J$	0	$J+\frac{1}{2}\Delta J$
$3z^2-r^2$	$J-\frac{5}{2}\Delta J$	$J-\frac{5}{2}\Delta J$	$J+\frac{1}{2}\Delta J$	$J+\frac{1}{2}\Delta J$	0

The index i refers to the five different basis orbitals of the canonical d bands in unit cell I and N denotes the number of unit cells. These atomic orbitals have been adapted to cubic symmetry, i.e., two are of e_g and three of t_{2g} character. The coefficients $\gamma_{mi}(\mathbf{k})$ are obtained from the eigenvectors of the corresponding canonical structure matrix given in Appendix A.

All interaction matrix elements V_{ijkl} depending on more than two different orbitals are neglected. Under this restriction the most general form of V_{ijkl} allowed by atomic symmetry[31] is

$$V_{ijkl} = U_{ik}\delta_{ij}\delta_{kl} + J_{ij}\delta_{il}\delta_{jk} + J_{ij}\delta_{ik}\delta_{jl}, \tag{4}$$

$$U_{ik} = U + 2J - 2J_{ik}. \tag{5}$$

The matrix elements J_{ij} depend upon two different parameters only, i.e., the exchange constant J and the anisotropy parameter ΔJ. They are listed in Table I.

For the following it will be useful to subtract from the interaction Hamiltonian H_1' the Hartree-Fock (HF) part H_1''. In addition, the canonical bands are assumed to be the result of a self-consistent field calculation. Therefore H_1'' will be absorbed in the definition of H_0. Thus the Hamiltonian is given by $H = H_0 + H_1$, where $H_0 = H_0'$ and

$$H_1 = H_1' - H_1'' + \tfrac{1}{2}\langle H_1''\rangle, \tag{6}$$

$$H_1'' = \sum_{I\sigma}\sum_{ijl}(2V_{ijll} - V_{illj})n_l d_{iI\sigma}^{\dagger} d_{jI\sigma}. \tag{7}$$

The expectation value $\langle \ldots \rangle$ in Eq. (6) is taken with respect to the ground state $|\Phi_0\rangle$ of H_0, in which all single-particle states are occupied by d electrons up to the Fermi energy ϵ_F. The term $\frac{1}{2}\langle H_1''\rangle$ ensures that $\langle H_1\rangle = 0$. Furthermore, $n_l = \langle d_{lI\sigma}^{\dagger} d_{lI\sigma}\rangle$ denotes the site occupation number of a single d orbital with index l.

By varying the Coulomb parameters U, J, and ΔJ and the total number of d electrons per site n_d, different transition-metal elements can be investigated. In the following the HF bandwidth W will be used as the unit of energy.

III. GROUND STATE

The starting point for the construction of the correlated ground state is the corresponding wave function $|\Phi_0\rangle$ of H_0. The Coulomb interaction is thereby taken into account only in mean-field approximation. A correlation hole, which shows up in particular in the pair-distribution function of electrons with opposite spins, cannot be described within that framework. It is common knowledge that one is able to treat electronic correlations quite accurately in atoms or molecules by applying quantum-chemical methods. Often they are based on a variational ansatz for the ground-state wave function, in which configurations with one- and two-particle excitations out of the HF ground state are superimposed on $|\Phi_0\rangle$ (configurational interaction). Therefore it seems natural to use a similar approach to the correlation problem in crystals.

A complication of calculations with variational wave functions for many-particle systems is their possible lack of size consistency. The ground-state energy E_0 of a system is an extensive quantity, which is proportional to the number of particles N_e in the system. In general, a variational calculation of the ground-state energy contains also statistically independent processes, which lead to unphysical terms proportional to higher powers in N_e. We circumvent this problem right from the beginning by using a formula for the ground-state energy E_0, which remains size consistent when various approximations are made. As was shown in Ref. 32 the following relation holds:

$$E_0 = (H|\Omega) = \left(H|1 + \lim_{x\to 0}\frac{1}{x - (\mathcal{L}_0 + H_1)}H_1\right). \tag{8}$$

Here the Liouville operator $\mathcal{L}_0$ acts as a superoperator on operators A according to the definition $\mathcal{L}_0 A = [H_0, A]_-$. Important in Eq. (8) is the formation of cumulants, which enters the definition of the round brackets and is abbreviated by the subscript c:

$$(A|B) = \langle A^{\dagger}B\rangle_c. \tag{9}$$

According to their definition cumulants eliminate all statistically independent processes from Eq. (8). A survey about properties and applications of cumulants can be found in Ref. 33. If Ω is expanded in powers of H_1 then E_0 represents the Rayleigh-Schrödinger perturbation series. If the expectation values in (8) contain only operators fulfilling fermionic anticommutation relations as in this work they can be evaluated by using Wick's theorem. In that case the formation of cumulants becomes equivalent to the prescription to consider exclusively connected diagrams. Equation (8) can be viewed as a generalization of Goldstone's linked cluster theorem[34] to cases where Wick's theorem does not apply.

The exact ground state of the system $|\Psi_0\rangle$ can be characterized by $|\Omega)$ as is suggested by Eq. (8). The operator Ω resembles the wave operator which transforms $|\Phi_0\rangle$ into $|\Psi_0\rangle$, the distinction being that here Ω appears only in connection with the metric form (9). The following ansatz is made:

$$|\Omega) = \left|1 - \sum_{\mu}\eta_\mu A_\mu\right). \tag{10}$$

Here the operators A_μ, $\mu = 1, \ldots, M$ describe different kinds of two-particle excitations. The coefficients η_μ are evaluated using the identity $(A|H\Omega) = 0$, which holds for arbitrary operators A (see Ref. 35). The relation seems plausible, since $|\Omega)$ replaces the exact ground state, which is an eigenstate of H. Therefore the corresponding expectation value factorizes for any operator A and the cumulant vanishes. If we use the ansatz (10) for Ω and set $A = A_\mu$ we obtain a system of linear equations, which determines the parameters η_μ:

$$\sum_{\nu}\eta_\nu(A_\mu|HA_\nu) = (A_\mu|H), \qquad \mu = 1, \ldots, M. \tag{11}$$

The Hamiltonian H_1 creates two important types of two-particle excitations on a lattice site I, namely spin excitations $\mathbf{S}_{iI}\,\mathbf{S}_{jI}$ and density excitations $n_{iI}n_{jI}$, where

$$\mathbf{S}_{iI} = \frac{1}{2}\sum_{\sigma\sigma'} d^{\dagger}_{iI\sigma}\boldsymbol{\sigma}_{\sigma\sigma'}d_{iI\sigma'}, \tag{12}$$

$$n_{iI} = \sum_{\sigma} n_{iI\sigma} = \sum_{\sigma} d^{\dagger}_{iI\sigma}d_{iI\sigma}. \tag{13}$$

In the first equation, $\boldsymbol{\sigma}$ denotes the usual Pauli spin matrices. As in the application of the local ansatz to transition metals by Stollhoff and Thalmeier[21] and Oleś and Stollhoff[22] we therefore introduce the following set of operators A_μ:

$$A^1_{ij}(I) = \begin{cases} 2\delta n_{iI\uparrow}\delta n_{iI\downarrow}, & i = j \\ \delta n_{iI}\,\delta n_{jI}, & i \neq j, \end{cases} \tag{14}$$

$$A^2_{ij}(I) = \mathbf{S}_{iI}\mathbf{S}_{jI}, \quad i \neq j. \tag{15}$$

Here, the multi-index μ has been replaced by $\mu = (t, i, j)$, where $t = 1, 2$ distinguishes between density and spin excitations and i, j are indices of atomic orbitals on site I. Furthermore, the ground-state expectation values of the density operators have been subtracted according to $\delta n = n - \langle n\rangle$. As a consequence the operators $A^t_{ij}(I)$ create exclusively two-particle excitations. In order to avoid redundancy we require $i \geq j$. The total number of correlation operators A_μ therefore equals $15 + 10 = 25$. The corresponding operators for the lattice are constructed by simply summing over the lattice sites: $A^t_{ij} = \sum_I A^t_{ij}(I)$.

As mentioned before the operators A_μ appear in the interaction Hamiltonian H_1. In terms of these operators H_1 is given by

$$H_1 = \frac{1}{4}\sum_{ij}[(2U_{ij} - J_{ij})A^1_{ij} - 4J_{ij}(A^2_{ij} + A^3_{ij})]. \tag{16}$$

The operators A^3_{ij}, which are ignored in the ansatz for the correlated ground state, transfer two electrons from orbital i to orbital j and vice versa:

$$A^3_{ij}(I) = \tfrac{1}{2}(\, d^{\dagger}_{iI\uparrow}d^{\dagger}_{iI\downarrow}d_{jI\uparrow}d_{jI\downarrow} + \text{H.c.}). \tag{17}$$

The described ansatz leads to a considerable reduction of charge fluctuations in comparison with the unperturbed ground state $|\Phi_0\rangle$ and to the formation of local moments. For details see Refs. 21 and 36.

When evaluating the expectation values for the ground state in local space hopping processes between different unit cells are neglected ($R = 0$ approximation[37]), i.e., it is assumed that $\langle d^{\dagger}_{iI\sigma}d_{jJ\sigma}\rangle = \delta_{IJ}\langle d^{\dagger}_{iI\sigma}d_{jI\sigma}\rangle$. This approximation corresponds to the neglect of momentum conservation when evaluating the diagrams in k-space representation and becomes exact in infinite dimensions.[38] In fact without it the calculation of third-order diagrams would not be possible since it would involve threefold integrations over a three-dimensional Brillouin zone. The error seems to be less than 5% in those cases where it can be checked. Consequently, it suffices to consider the interaction processes within a single transition-metal atom in unit cell I. The matrix elements in Eq. (11) depend only on the parameters U, J, and ΔJ, the orbital energies e_i and the occupation numbers n_i (see Appendix B).

IV. EXCITED STATES

Having described the correlated ground state of our model system we now turn to its excitation spectrum. The one-particle excitations of d electrons may be calculated by considering the corresponding retarded Green's functions $G_{\mu\nu}(\mathbf{k}, t)$, which are defined as

$$G_{\mu\nu}(\mathbf{k}, t) = -i\theta(t)\langle\Psi_0|[B^{\dagger}_{\mu}(\mathbf{k}, t), B_\nu(\mathbf{k}, 0)]_+|\Psi_0\rangle. \tag{18}$$

Here $B^{\dagger}_{\mu}(\mathbf{k}, t)$, $B_\nu(\mathbf{k}, 0)$ denote arbitrary operators in the Heisenberg picture, $\theta(t)$ is the step function, and $|\Psi_0\rangle$ represents the exact ground state. If we replace $B^{\dagger}_{\mu}(\mathbf{k}, t)$ and $B_\nu(\mathbf{k}, 0)$ by $d_{m\mathbf{k}\sigma}(t)$ and $d^{\dagger}_{m\mathbf{k}\sigma}$, respectively, the excitation spectrum of the corresponding type of d electron can be determined from the imaginary part of the retarded Green's function.

As in the previous section we choose a formulation which is inherently size consistent. It has been shown by Becker and Brenig[39] that the Laplace transform of $G_{\mu\nu}(\mathbf{k}, t)$ can be written in terms of cumulants as

$$G_{\mu\nu}(\mathbf{k}, \omega) = \left(\Omega\left|\left[B^{\dagger}_{\mu}(\mathbf{k}), \frac{1}{\omega - \mathcal{L}}B_\nu(\mathbf{k})\right]_+\right|\Omega\right). \tag{19}$$

Thereby $\mathcal{L}$ represents the Liouville operator of H. It should be mentioned that the expression $[\omega - \mathcal{L}]^{-1}B_\nu(\mathbf{k})$ has to be viewed as an entity when cumulants are formed. As before the exact ground state $|\Psi_0\rangle$ has been replaced by $|\Omega\rangle$.

Equation (19) is in a proper form to be evaluated by the projection technique of Mori[27] and Zwanzig.[28] Thereby the propagator $[\omega - \mathcal{L}]^{-1}$ is projected onto a relevant operator space spanned by the set $\mathcal{R} = \{B_1, ..., B_M\}$. Within this space the dynamics is treated exactly. If one neglects the influence of the remaining part of the operator space the matrix $\underline{G}$ of correlation functions within the relevant set $\mathcal{R}$ is given by

$$\underline{G}(\mathbf{k}, \omega) = \underline{X}\,[\,\omega\underline{X} - \underline{F}\,]^{-1}\underline{X}. \tag{20}$$

For a derivation see Forster.[40] Two quantities enter the projection equation (20), namely, the frequency matrix $\underline{F}$ and the susceptibility matrix $\underline{X}$:

$$F_{\mu\nu} = (\Omega|\,[B^{\dagger}_{\mu}, \mathcal{L}B_\nu]_+\,\Omega), \tag{21}$$

$$X_{\mu\nu} = (\Omega|\,[B^{\dagger}_{\mu}, B_\nu]_+\,\Omega). \tag{22}$$

As before, $\mathcal{L}B_\nu$ has to be treated as an entity with respect to cumulant formation. In Eqs. (21) and (22) the correlated ground state will be approximated by inserting the ansatz of Eq. (10) for $|\Omega\rangle$.

The final step in the calculation of the excitation spectrum for transition metals consists in the proper choice of the relevant operator set $\mathcal{R}$. Obviously, the operator $d^{\dagger}_{m\mathbf{k}\sigma}$ itself has to be included in that set since one is interested in its spectrum. Operators coupling to $d^{\dagger}_{m\mathbf{k}\sigma}$ are found as in the usual equation-of-motion method by considering the commutator $\mathcal{L}_1 d^{\dagger}_{m\mathbf{k}\sigma}$, where $\mathcal{L}_1$ represents the Liouville operator of H_1. We choose the following relevant operator set $B_\mu(m, \mathbf{k})$ which is directly related

to the two-particle excitation operators of the ground state A_μ:

$$B^0(m,\mathbf{k}) = d^\dagger_{m\mathbf{k}\uparrow}, \tag{23}$$

$$B^t_{ij}(m,\mathbf{k}) = N^{-\frac{1}{2}} \sum_I e^{-i\mathbf{k}\cdot\mathbf{R}_I} [A^t_{ij}(I), d^\dagger_{iI\uparrow}]_-. \tag{24}$$

According to their definition the operators $B^t_{ij}(m,\mathbf{k})$ consist of a lattice sum over local operators $B^t_{ij}(I) = [A^t_{ij}(I), d^\dagger_{iI\uparrow}]_-$. At a given site I the local operators create an additional electron which is accompanied by one-particle excitations of spin and density type:

$$B^1_{ij}(I) = \begin{cases} 2d^\dagger_{iI\uparrow}\delta n_{iI\downarrow}, & i=j \\ d^\dagger_{iI\uparrow}\delta n_{jI}, & i\neq j, \end{cases} \tag{25}$$

$$B^2_{ij}(I) = \tfrac{1}{2}(d^\dagger_{iI\uparrow}S^z_{jI} + d^\dagger_{iI\downarrow}S^+_{jI}), \quad i\neq j, \tag{26}$$

$$B^3_{ij}(I) = \tfrac{1}{2}\, d^\dagger_{jI\downarrow}d^\dagger_{jI\uparrow}d_{iI\downarrow}, \quad i\neq j. \tag{27}$$

In Eq. (26) $S^z_{jI} = \frac{1}{2}(n_{jI\uparrow} - n_{jI\downarrow})$ is the z component of the d electron spin operator for orbital j and $S^+_{jI} = d^\dagger_{jI\uparrow}d_{jI\downarrow}$ represents the corresponding spin-flip excitation. The total number of operators $B_\mu(m,\mathbf{k})$ for fixed band index m and wave vector $\mathbf{k}$ equals $1+25+20+20=66$.

As in the ground-state calculation we apply the $R=0$ approximation to the frequency matrix elements of the one-particle Hamiltonian H_0 in order to avoid twofold integrations over the three-dimensional Brillouin zone. Furthermore, all those expectation values have been neglected which contain products of more than three operators of the form H_1, A^t_{ij}, or B^t_{ij} for $t=1,2,3$. The results for the frequency and susceptibility matrices as well as further details of the calculation can be found in Appendix C.

Finally, the connection of the present approach with Kanamori's t-matrix approximation as well as second-order perturbation theory should be discussed briefly. If we replace in Eq. (24) the local d operators by their Fourier transforms the operators $B^t_{ij}(m,\mathbf{k})$ can also be viewed as double k sums over operators which create three-particle states consisting of two d electrons and one d hole. When one omits the double summations and uses instead of the $B^t_{ij}(m,\mathbf{k})$ these three-particle operators depending on three different momenta directly as projection operators the calculation becomes equivalent to a complete solution of a three-particle scattering problem in k space. Starting from these equations Kanamori's t-matrix approximation is derived in the low-density limit by taking only the multiple hole-hole scattering processes[41] (ladder diagrams) into account. However, in order to go beyond the low-density limit one has to consider the electron-hole scattering channel as well. Second-order perturbation theory is obtained if one neglects the Coulomb interaction in the frequency matrix elements of the three-particle operators completely, i.e., if one replaces $\mathcal{L}$ by $\mathcal{L}_0$ in Eq. (21).

For a one-band Hubbard model describing the case of strongly ferromagnetic Ni the complete three-particle scattering problem can be solved,[13] which leads to quite accurate excitation spectra. Since it is impossible to solve the corresponding problem for a Hamiltonian containing multiplet splittings as in the present work, the substitution of the general three-particle operators by the integrated versions $B^t_{ij}(m,\mathbf{k})$ is reasonable as long as the number of charge carriers is not too high. However, near half filling this local approach is not applicable any more for the excitation spectra. (For tests of the accuracy of the local approximation, see Ref. 42.)

V. GROUND-STATE PROPERTIES AND PARAMETER VALUES

In the ansatz (10) for the correlated ground-state density and spin excitations are added to the HF state, which considerably lowers the ground-state energy E_0. For a local Coulomb repulsion of $U=0.5$ and half filling ($n_d=5$), for example, the correlation energy $E_c = E_0 - E_{\mathrm{HF}}$ amounts approximately to 30% of the HF ground-state energy E_{HF}. Away from half filling the relative contribution of E_c becomes smaller and finally vanishes for empty or completely filled bands.

Furthermore, ground-state correlations drastically reduce charge fluctuations on single transition-metal ions in the lattice. If $N = \sum_{i\sigma} n_{iI\sigma}$ denotes the local particle number operator the expectation value for charge fluctuations is given by $\langle \delta N^2\rangle = \langle N^2\rangle - \langle N\rangle^2$. It is shown in Fig. 1 with respect to the correlated (full lines) or uncorrelated ground state (dashed lines) for (a) the fcc and (b) the bcc structure. As a result of correlation effects the local occupation number fluctuates only between $n_d \pm 1$.

Finally, results for the total effective moments $\langle \mathbf{S}^2\rangle$ with $\mathbf{S} = \sum_i \mathbf{S}_{iI}$ are presented in Figs. 1(c) and 1(d) for the fcc and bcc structure, respectively. The large in-

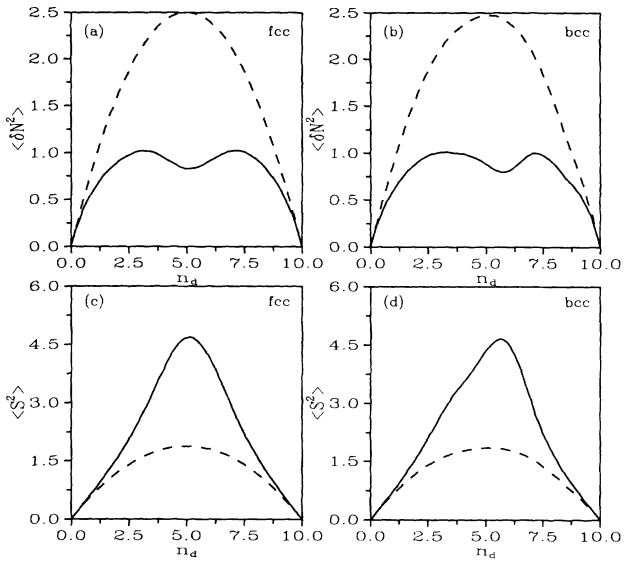

FIG. 1. (a) Charge fluctuations $\langle \delta N^2\rangle$ as a function of electron number n_d in the correlated ground state (full line) in comparison with the HF state (dashed) for the fcc structure. (b) The same for the bcc structure. (c) In contrast to the reduction of the charge fluctuations the total effective moment $\langle S^2\rangle$ clearly increases in the correlated state (full line) as compared with the HF state (dashed) in a fcc structure. (d) The same as in (c) but for the bcc structure. The parameter values are $U=0.5$, $J=0.12$, and $\Delta J = 0.017$ for all figures (a)–(d).

crease in the expectation values for the correlated state (full lines) as compared with the HF ground state (dashed lines) reflects the formation of local moments. For a parameter set of $U = 0.5$, $J = 0.12$, and $\Delta J = 0.017$ as in Fig. 1 one is approximately halfway between the uncorrelated values and the maximum spin polarization predicted by the first Hund's rule.

Before we turn to the presentation of the calculated excitation spectra we discuss the choice of the parameters U, J, and ΔJ, for the series of $3d$ transition metals. As mentioned before the simplified canonical bands, which are used in the present work, solely depend upon the crystal structure and the bandwidth W. The HF bandwidths are determined from the relation $W = c\mu^{-1}s^{-2}$, where μ is called the intrinsic band mass and s is the atomic sphere radius. Values for μ and s for different $3d$ transition metals can be found in Ref. 44. The constant c is fixed by assuming a bandwidth of 4.3 eV in the case of Ni. The spin-averaged LDA bandwidth of Ni has been taken from Ref. 46. As can be seen from Table II the $3d$ band width W slightly increases from Sc to V and then constantly drops up to Ni.

The Coulomb parameters U, J, and ΔJ are simple linear combinations of the Slater-Koster integrals F^0, F^2, and F^4, which have been tabulated for various kinds of atoms. However, in a solid the conduction electrons screen heavily the local Coulomb repulsion of the $3d$ electrons thereby reducing the values of F^0 by more than a factor of 10. (In the case of the integrals F^2 and F^4 there is only a reduction of 10%–20%.) Since an accurate inclusion of the screening effect is difficult the best choice is to take the parameter values directly from experiments. By measuring the multiplet structure of transition-metal ions embedded in simple metallic hosts like Cu or Ag the screened Coulomb parameters can be obtained directly. This way van der Marel and Sawatzky[45] deduced interpolation formulas for F^0, F^2, and F^4 which lead in our case to the parameter set

$$U = 1.22 + 0.174(Z - 21), \tag{28}$$

$$J = 0.49 + 0.062(Z - 21), \tag{29}$$

$$\Delta J = J/7. \tag{30}$$

Here, the energies of U and J are given in eV and Z is the atomic number of a $3d$ transition metal element. The resulting parameter values in units of the bandwidth W are also listed in Table II. As expected, the Coulomb repulsion U has its maximum value for Ni and decreases for Co, Fe down to V.

VI. EXCITATION SPECTRUM OF NI

The electronic excitation spectrum of Ni has been computed numerically by using the experimentally determined parameter set of Table II. The results are shown in Fig. 2. The spectrum is divided into a renormalized one-particle density of states of fcc form between -0.5 and 0.5 (in units of the HF bandwidth W) and a multiplet structure below -0.5, which contains 14% of the total weight. Obviously, the width of the quasiparticle band structure has been reduced by 15% as a consequence of correlation effects. The position of the Fermi energy is marked by a dotted line. Furthermore, the center of gravity of the canonical band structure has been taken as the zero point of energy.

For the chosen parameter set we find the maximum of the satellite structure at -1.16, approximately $1.57W = 6.75$ eV below the top of the d bands. This value is in good agreement with photoemission experiments, in which the center of the multiplet structure has been observed[2] around 6.3 eV. Angle-resolved photoemission experiments also reveal a strong reduction of the Ni bandwidth, where a spin-averaged value of 3.4 eV has been found[2,3] by several groups. When compared with the LDA width[46] of 4.3 eV this implies a reduction of 20%.

Due to the ferromagnetic polarization of Ni there is an exchange splitting between majority and minority spin bands. In optical experiments[2] a splitting of approximately 0.3 eV at the Fermi energy ϵ_F has been observed. The energy differences between majority and minority spin states decrease as one goes to lower-lying states and cannot be resolved any more at the bottom of the d bands. Spin-polarized LDA calculations, however, overestimate the exchange splittings and find values around 0.8 eV near ϵ_F. Therefore, if one compares the total spin-split d bandwidth of LDA calculations with experiments the reduction is even larger, i.e., around 30%. Such high reduction factors can also be obtained for the param-

TABLE II. Parameter values for the series of $3d$ transition metals. The respective HF bandwidths W have been derived by using data of Andersen and Jepsen (Ref. 29) for canonical band structures. The parameter values for U, J, and ΔJ in units of the bandwidths W are based on optical measurements (Ref. 45). In the bottom line the crystal structures of the $3d$ transition-metal elements are listed.

	Sc	Ti	V	Cr	Mn	Fe	Co	Ni
n_d	2.2	3.4	4.4	5.4	6.3	7.4	8.4	9.4
W (eV)	5.8	6.9	7.7	7.5	6.4	5.5	4.9	4.3
U (W)	0.20	0.20	0.20	0.23	0.30	0.38	0.45	0.56
J (W)	0.08	0.08	0.08	0.09	0.12	0.15	0.17	0.22
ΔJ (W)	0.012	0.011	0.011	0.013	0.017	0.021	0.025	0.031
str.	hcp	hcp	bcc	bcc	sc	bcc	fcc	fcc

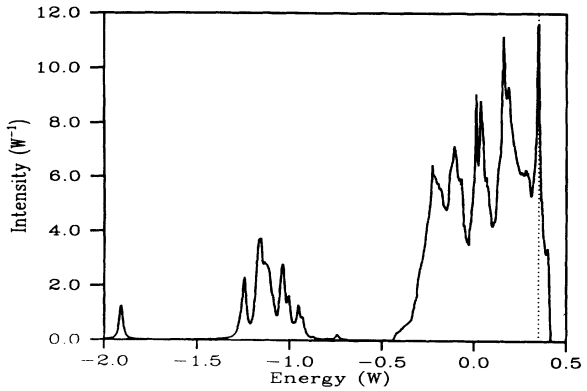

FIG. 2. Single-particle excitation spectrum of Ni for the parameter values $U = 0.56$, $J = 0.22$, $\Delta J = 0.031$, and an electron number of $n_d = 9.4$. The position of the Fermi energy is denoted by a dotted line. Energy is measured in units of the HF bandwidth W.

agnetic case when the comparably large paramagnetic LDA bandwidth of 4.8 eV from Moruzzi, Janak, and Williams[47] is used as reference value. Finally, it should be mentioned that the neglected $4s$ band of Ni leads to a rather flat density of states extending from −9 eV below ϵ_F up to 2 eV above ϵ_F. This constant background should simply be added to the spectrum of Fig. 2.

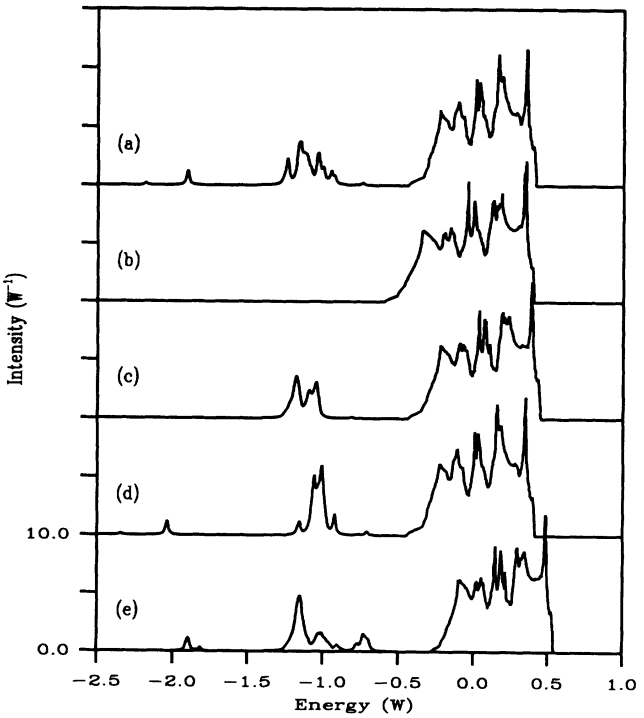

FIG. 3. Analysis of the Ni spectrum. (a) Full excitation spectrum of Ni for the parameters $U = 0.56$, $J = 0.22$, $\Delta J = 0.031$ as in Fig. 2; (b) HF density of states for the fcc structure; (c) spectrum for $U = 0.56$, $J = \Delta J = 0$; (d) spectrum for $U = 0.56$, $J = 0.22$, $\Delta J = 0$; (e) excitation spectrum of Ni for parameters as in (a) but without ground-state fluctuations taken into account.

In conclusion, the experimental parameters of Ref. 45 lead to the correct satellite position but the obtained reduction of 15% is somewhat too small. However, such a relatively weak band renormalization has also been found in exact diagonalization studies[19] and in calculations based on Kanamori's t-matrix theory.[10–17] Therefore it seems to be a deficiency of the simplified model Hamiltonian rather than of the approximation scheme used. The inclusion of Coulomb interactions between neighboring ions, for example, increases the band narrowing whereas the satellite position is not changed very much, as has been pointed out by Aisaka *et al.*[48]

In order to obtain more insight into the composition of the multiplet structure we show in Fig. 3 the Ni spectrum for different choices of the parameter sets. By comparing the HF density of states for the fcc lattice in Fig. 3(b) with the full Ni spectrum of Fig. 3(a) it becomes apparent that the shape of the quasiparticle density of states above −0.5 remains the same when correlation effects are included. There is only a reduction of bandwidth. In Fig. 3(c) the Ni spectrum is presented for $U = 0.56$, but without exchange interactions, i.e., for $J = \Delta J = 0$. In this case there is only one quasiparticle and one satellite peak at each k point for fixed band index m. For that reason the shape of the multiplet structure just reflects the flat dispersion of the satellite peaks and their e_g-t_{2g} splitting due to the cubic ligand field.

Upon turning on the J parameter two new features appear in Fig. 3(d) near −2.1 and −0.7, respectively, beside the main structure around −1.1. The shape of the spectrum reflects the form of the atomic d^2 multiplet for the same parameters, which shows a splitting into three peaks corresponding to a ^1S state, the degenerate singlet states ^1G,^1D, and the degenerate triplet states ^3P,^3F. The energy difference between ^1S and ^1G equals $5J$ and there is a singlet-triplet splitting of $2J$ between ^1G and ^3F. The three structures at −2.1, −1.1, and −0.7 show a comparable energy spacing. Furthermore, the states at −2.1 and −1.1 are mainly of singlet character, whereas the peak at −0.7 has triplet character. The singlet (triplet) character of the structures in the spectrum can be checked by looking at the spectral weight distribution of the operators $B^1_{ij}-4B^2_{ij}$ ($B^1_{ij}+4B^2_{ij}$), which create predominantly singlet (triplet) states for low carrier concentrations. Finally, the anisotropy parameter ΔJ splits the main structure around −1.1 into smaller substructures as can be seen by going back to Fig. 3(a).

The plot Fig. 3(e) presents the Ni spectrum for the complete parameter set of Table II but without ground-state fluctuations, i.e., the η parameters in Eq. (10) have been set equal to zero. In this case the weight of the states around −0.75 with triplet character is much higher. Obviously, ground-state fluctuations have the tendency to lower the weight of the triplet states. Furthermore, the reduction of the bandwidth equals 18% without ground-state fluctuations, a value which shrinks to 15% when the full ground-state ansatz is used.

By looking at the parameter dependence of the satellite structure in the Ni spectrum its relation to an atomic d^2 multiplet becomes apparent. However, the detailed shape of the peaks especially within the main structure

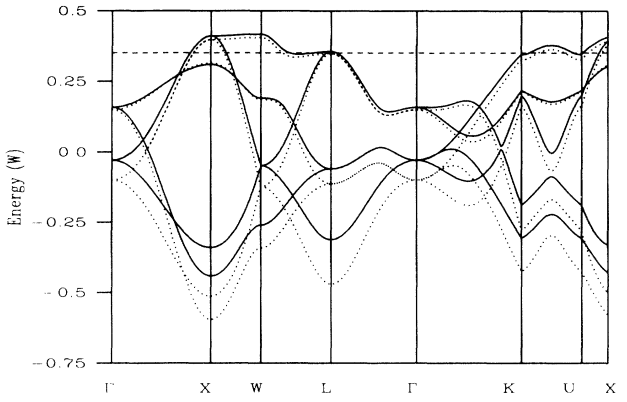

FIG. 4. Renormalized quasiparticle bands of fcc Ni (full lines) in comparison with the HF band structure (dotted) along lines of high symmetry in the Brillouin zone. The dashed line shows the position of the renormalized Fermi energy. Parameters are the same as in Fig. 2.

is clearly affected by the dispersion of the satellite peaks as well as by the e_g-t_{2g} splittings. The spectrum deviates in this region from a simple atomic picture.

Figure 4 shows the dispersion of the five canonical d bands for the fcc structure (dotted lines) together with the renormalized band structure of Ni (full lines) along directions of high symmetry in the Brillouin zone. The dashed line marks the position of the Fermi level. Obviously, there is no change in the shape of the band structure, i.e., the renormalized bands are just quenched by 15%. The shift of the bands is strongest at the bottom of the d bands and is constantly decreasing up to the Fermi energy.

In Fig. 5 the corresponding curves are shown for the bcc structure thereby using the same parameters as in the previous figure. Also in this case the shape of the bands remains unaffected by correlations. There is only a slight perturbation of the renormalized bands near the H point due to satellite peaks which appear in an energy region of -0.4 up to -0.3. The reduction of the bandwidth equals 11%, somewhat smaller than in the fcc case.

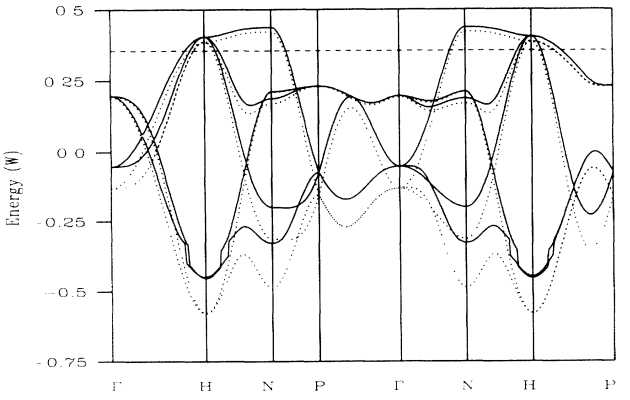

FIG. 5. Renormalized quasiparticle bands for the bcc structure (full lines) in comparison with the HF band structure (dotted). The position of the Fermi energy is marked by a dashed line. Parameters are the same as in Fig. 4 (bcc Ni).

VII. 3D TRANSITION-METAL SERIES

In the following section the dependence of the excitation spectrum on the electron number n_d will be discussed. In Fig. 6 a series of transition metals with fcc structure is presented with the following electron numbers: (a) $n_d = 9.4$ corresponding to Ni, (b) $n_d = 8.4$ corresponding to Co, (c) $n_d = 2.2$ corresponding to Sc, and (d) $n_d = 0.6$. Figure 7 shows the spectra for bcc metals with (a) $n_d = 9.4$, (b) $n_d = 7.4$ corresponding to Fe, (c) $n_d = 1.6$, and (d) $n_d = 0.6$. In the cases of Co and Fe the exchange parameters J, ΔJ have been reduced as compared with the experimental values of Table II in order to lower the satellite weights. Furthermore, Sc has a hcp structure in reality but the overall shape of the one-particle density of states differs not very much from that of the fcc structure.

Apparently, the spectra show some kind of electron-hole symmetry: For $n_d > 5$ a multiplet structure appears on the low-energy side of the photoemission spectrum and for $n_d < 5$ on the high-energy side of the inverse photoemission spectrum. Increasing the number of charge carriers, i.e., holes in the first case and electrons in the latter, results in an increase of the spectral weights of the satellite structures. Especially the triplet peaks grow appreciably. Simultaneously the reduction of the bandwidth becomes more pronounced. The weight of the satellite structure in Fig. 7(b) for Fe is stronger than in Fig. 7(a) although the Coulomb repulsion U has been lowered from $U = 0.56$ to $U = 0.38$. Obviously, the influ-

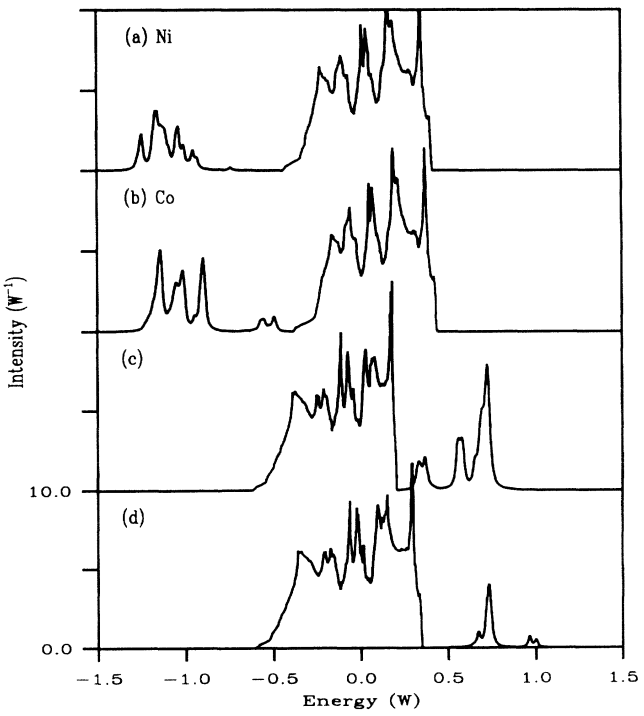

FIG. 6. Series of 3d transition metals with fcc structure: (a) Ni spectrum, $n_d = 9.4$, $U = 0.56$, $J = 0.22$, $\Delta J = 0.031$; (b) Co spectrum, $n_d = 8.4$, $U = 0.45$, $J = 0.10$, $\Delta J = 0.015$; (c) "Sc" spectrum, $n_d = 2.2$, $U = 0.20$, $J = 0.08$, $\Delta J = 0.012$; (d) spectrum for $n_d = 0.6$, $U = 0.20$, $J = 0.08$, $\Delta J = 0.01$.

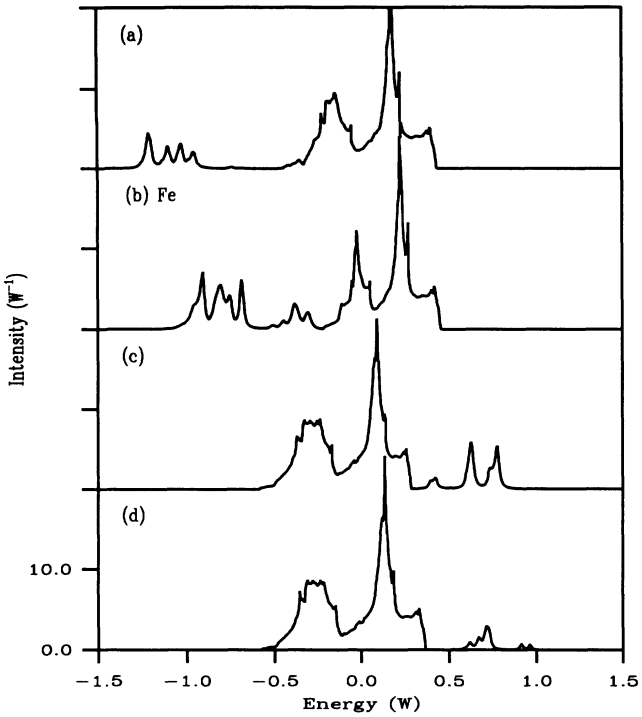

FIG. 7. Series of 3d transition metals with bcc structure: (a) Spectrum for $n_d = 9.4$, $U = 0.56$, $J = 0.22$, $\Delta J = 0.031$; (b) Fe spectrum, $n_d = 7.4$, $U = 0.38$, $J = 0.10$, $\Delta J = 0.015$; (c) spectrum for $n_d = 1.6$, $U = 0.20$, $J = 0.08$, $\Delta J = 0.01$; (d) spectrum for $n_d = 0.6$, $U = 0.20$, $J = 0.08$, $\Delta J = 0.01$.

ence of the charge-carrier concentration is the dominating effect. In conclusion, the present model Hamiltonian treated by the local ansatz distinctly predicts satellite structures and band narrowing also for Co, Fe, and Sc.

A reduction of the LDA bandwidth has indeed been found experimentally[1] for Co (about 20%) as well as for Fe (about 10%). However, photoemission measurements clearly reveal that correlation effects become weaker if one goes from Ni to Co to Fe in contradiction with our findings. Furthermore, there is no convincing evidence for atomiclike multiplet structures in these transition metals, although their weight increases in our model calculation from Ni to Co and Fe.

The ratio of the correlated to the HF bandwidth W_r/W as a function of electron number n_d is shown in Fig. 8 for the three different Coulomb parameters $U = 0.5$, $U = 0.3$, and $U = 0.2$. Lowering the Coulomb strength certainly increases the bandwidth. But in the case of Fe there is still a reduction of 29% for $U = 0.2$. Similar findings hold for the share of the satellite weight I_s with respect to the total weight I_t, which is shown in Fig. 9 for the same parameter sets as in the previous figure. Also in that case the increase in the number of charge carriers (holes) clearly enhances the satellite weight. For that reason even a drastic reduction of the Coulomb parameters cannot eliminate the fundamental discrepancies.

The existence of multiplet structures in the photoemission spectra of Co and Fe has also been predicted in earlier works for similar model Hamiltonians by applying the t-matrix approach[10,11] or second-order perturbation theory.[8] The local approach used in the present calculation takes all three-particle scattering diagrams into account, i.e., it includes the second-order perturbation theory as well as the series of ladder diagrams of the t-matrix approach. Furthermore, a correlated ground state has been used as starting point instead of a simple HF state. On the other hand the scattering processes have been treated in an integrated fashion due to the use of local excitation operators $B^t_{ij}(I)$ as pointed out at the end of Sec. IV. Consequently, the peaks in the excitation spectra show no damping effects. In Ref. 42 it has been demonstrated that the local approach is quite accurate for low carrier concentrations as in the case of Ni. With increasing electron or hole density, however, the neglected broadening of the satellite and quasiparticle peaks becomes more important. Therefore one can expect that instead of the discrete peaks in the multiplet structure of Fe in Fig. 7 one would just obtain a broad hump. In addition, the broadening of the δ peaks would increase the quasiparticle bandwidth and lower the satellite weights. Nevertheless, due to our model Hamiltonian clear multiplet structures should be found experimentally in Co

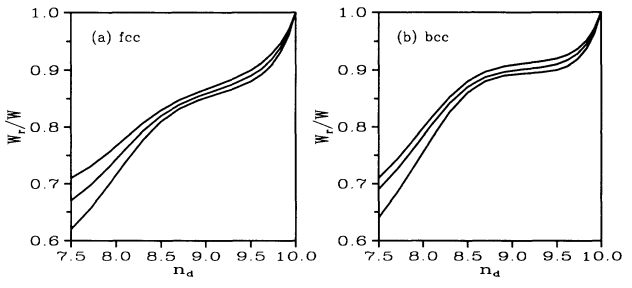

FIG. 8. (a) Ratio between the renormalized bandwidth W_r and the HF bandwidth W as a function of electron number n_d for the fcc structure. The three curves refer from top to bottom to the parameter sets ($U = 0.2$, $J = 0.06$, $\Delta J = 0.008$), ($U = 0.3$, $J = 0.1$, $\Delta J = 0.015$), and ($U = 0.5$, $J = 0.1$, $\Delta J = 0.015$). (b) The same for the bcc structure.

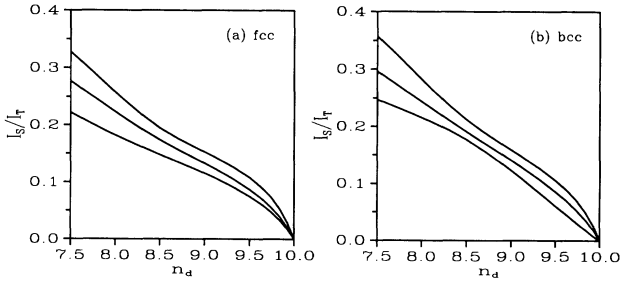

FIG. 9. Ratio between the spectral weight of the satellite structure I_s and the total spectral weight I_t as a function of electron number n_d for the fcc structure: Starting with the topmost full line the three curves have been calculated using the parameter sets ($U = 0.5$, $J = 0.1$, $\Delta J = 0.015$), ($U = 0.3$, $J = 0.1$, $\Delta J = 0.015$), and ($U = 0.2$, $J = 0.06$, $\Delta J = 0.008$) as in Fig. 8. (b) The same for the bcc structure.

and Fe just as in Ni provided that the chosen parameter values of Table II are applicable. However, if the values of the Coulomb parameters U and J are lowered drastically the broadening of the quasiparticle peaks leads to qualitative changes. For example, in the case of Ni the satellite structure disappears for $U < 0.2$ in second-order perturbation theory.[8]

There is another feature which lowers the satellite weights in the photoemission spectra of Co and Fe. Second-order perturbation theory shows the existence of a second multiplet structure at the high-energy edge of the inverse photoemission spectrum. The spectral intensity of this satellite increases with increasing charge-carrier concentration. For Ni it has practically no weight but in case of Fe about 25% of the total satellite intensity will be transferred to the inverse spectrum. In order to obtain this structure in a local approach one has to extend the set of projection operators $B^t_{ij}(I)$. For that purpose the local creation operator of a d electron in orbital i at site I is decomposed into $d^\dagger_{iI\sigma} = \bar{d}^\dagger_{iI\sigma} + \hat{d}^\dagger_{iI\sigma}$, where

$$\bar{d}^\dagger_{iI\sigma} = N^{-\frac{1}{2}} \sum_{m\mathbf{k}} \Theta(\epsilon_F - \epsilon_{m\mathbf{k}}) e^{i\mathbf{k}\cdot\mathbf{R}_I} \gamma^*_{mi}(\mathbf{k})\, d^\dagger_{m\mathbf{k}\sigma}. \tag{31}$$

The distinction of the two types of local operators $\bar{d}^\dagger_{iI\sigma}$ and $\hat{d}^\dagger_{iI\sigma}$ leads to two new operator sets $\hat{B}^t_{ij}(I)$ and $\bar{B}^t_{ij}(I)$ (corresponding to the operator combinations $\hat{d}^\dagger\hat{d}^\dagger\bar{d}$ and $\bar{d}\bar{d}\hat{d}^\dagger$, respectively). They produce satellite structures at both edges of the quasiparticle density of states of the d electrons. Note that the use of the described operator sets is complicated by the fact that the creation and annihilation operators of Eq. (31) at different lattice sites do not anticommute any longer. Although the second multiplet structure will reduce the spectral weight of the satellite in the photoemission spectrum it will not alter the strong band narrowing of Fe.

VIII. DISCUSSION AND SUMMARY

Having discussed the advantages and disadvantages of a local approach to the correlation problem in transition metals we consider the limitations of our model. In the HF part of the Hamiltonian the most serious deficiency is the neglect of the $4s$ electrons. The detailed form of the $3d$ bands is clearly altered due to hybridization with the $4s$ band. If the $4s$ states are included in (1) and the canonical band structures are scaled carefully for each transition metal element they deviate only by a few percent of the total bandwidth from accurate self-consistent field calculations. The HF results influence the correlation calculation by the form of the dispersion curves $\epsilon_{m\mathbf{k}}$ and the occupation numbers n_i of the $3d$ orbitals. With respect to the occupation numbers the effect of the hybridization between $3d$ and $4s$ electrons has already been taken into account by using the correct values of the d electron numbers n_d in the calculation. Therefore the inclusion of the $4s$ electrons will mainly lead to a rather flat and extended background in the excitation spectra. For these reasons we can conclude that improvements on the HF level will not cause qualitative changes of the presented results.

With respect to the interaction part of the model Hamiltonian the situation is different. Here the dynamically screened interaction W between $3d$ electrons in transition metals has been replaced by a static intra-atomic Coulomb interaction V. The frequency dependence as well as the k dependence of W are approximated by a constant. The intra-atomic interactions between electrons in the five $3d$ orbitals are sufficiently described by our model Hamiltonian. For symmetry reasons they are determined by the three Slater-Koster integrals F^0, F^2, and F^4 so that the absolute values of these parameters for different transition-metals are the only unknown quantities here. Interatomic interactions between neighboring transition-metal ions, however, can influence the excitation spectra even if the interaction strengths are small since the number of nearest neighbors is high in these closely packed solids.

If one considers the screening of $3d$ holes in transition metals one expects qualitative differences between Ni and Co or Fe since a hole in a Ni ion is only screened by $4s$ electrons whereas in Co or Fe also the other $3d$ holes within the same ion participate in the screening. Therefore, the screened interaction W could be considerably weaker in Co or Fe than in Ni. However, these considerations are in conflict with the experimental results of van der Marel and Sawatzky.[45] Furthermore, the ferromagnetic phase becomes unstable if the Coulomb parameters U and J are drastically lowered for Co and Fe.[22]

The dominating frequency dependence of the screened interaction W results from plasmon excitations, which appear 25 eV below the Fermi energy in Ni. These plasmon poles in connection with a continuum of single-particle excitations reduce the HF bandwidth of Ni by about 20% when the Fock diagram is replaced by a screened exchange.[6] The 6 eV satellite of Ni, however, is missing in the GW calculation. As has been shown in Sec. VI this satellite structure will further narrow the bandwidth of Ni by 15%. By combining both effects a measured reduction of 30% of the d band width in Ni (including spin splitting) can be understood. It would be interesting to perform similar GW calculations also for Co and Fe in order to obtain better insight into the form of the screened interaction between $3d$ electrons in these materials.

In conclusion we have calculated the electronic single-particle spectrum of $3d$ transition metals for a model Hamiltonian, which includes realistic d band structures (fcc and bcc) as well as all relevant Coulomb matrix elements between the five d orbitals at a given site. Using experimental values for the Coulomb parameters, the correct position of the satellite structure in the photoemission spectrum of Ni has been obtained. The band narrowing by 15% is smaller than the experimental value. This discrepancy is reasonable since the dynamical screening of the Coulomb interaction in the first-order exchange diagram leads to an additional reduction by the same amount. The numerical calculations also predict pronounced multiplet structures in the spectra of Co and Fe for Coulomb parameters determined by optical exper-

iments. Their absence in photoemission measurements raises the question whether a model with static intra-atomic Coulomb interactions between d electrons contains the essential physics of all of the 3d transition-metal elements.

ACKNOWLEDGMENTS

We would like to thank G. Stollhoff for valuable discussions. One of the authors (P. U.) would like to thank the Gunma University Foundation for Science and Technology for financial support.

APPENDIX A: CANONICAL BANDS

The dispersion relations $\epsilon_{m\mathbf{k}}$ $(m=1,\ldots,5)$ of the five d bands in H_0 are obtained by diagonalizing the canonical structure matrices $\underline{S}(\mathbf{k})$ for a bcc or fcc lattice:

$$S_{ij}(\mathbf{k}) = \frac{g_{ij}}{\sqrt{4\pi}} \sum_{I\neq 0} e^{i\mathbf{k}\cdot\mathbf{R}_I} Y_{4(i-j)}\left(\frac{\mathbf{R}_I}{|\mathbf{R}_I|}\right)\left(\frac{s}{|\mathbf{R}_I|}\right)^5 , \tag{A1}$$

$$g_{ij} = (-1)^{i+1}\frac{10}{3}\frac{[(4+i-j)!(4-i+j)!]^{\frac{1}{2}}}{[(2+i)!(2-i)!(2+j)!(2-j)!]^{\frac{1}{2}}} . \tag{A2}$$

The index i refers to spherical harmonics Y_{li} with orbital momentum $l=2$ as basis functions. Furthermore, $s=(3V/4\pi)^{\frac{1}{3}}$ is the radius of the atomic sphere, which has the same volume V as the unit cell.

The canonical structure matrix depends exclusively upon the crystal structure and the only free parameters of the five resulting d bands are their total width W as well as their center of gravity, which we choose as the zero point of energy. For further details see Refs. 29 and 30.

APPENDIX B: GROUND STATE

In order to determine the correlated ground state the coefficients η_μ in Eq. (10) have to be calculated. For convenience we introduce the matrices

$$L^{st}_{ijkl} = (A^s_{ij}|HA^t_{kl}), \tag{B1}$$

$$M^t_{ij} = (A^t_{ij}|H). \tag{B2}$$

By inverting Eq. (11) we obtain a relation of the form

$$\eta^s_{ij} = \sum_{tkl}[L^{-1}]^{st}_{ijkl}M^t_{kl}. \tag{B3}$$

The matrix elements depend upon local occupation numbers n_i and orbital energies $e_i = E_i/n_i$. The hole occupation numbers are denoted by $\overline{n}_i = 1-n_i$. Furthermore, the orbital energy of a hole $\overline{e}_i$ is given by $\overline{e}_i = \overline{E}_i/\overline{n}_i$, where $\overline{E}_i(n_d) = E_i(10) - E_i(n_d)$ and

$$n_i = N^{-1}\sum_{m\mathbf{k}}\theta(\epsilon_F-\epsilon_{m\mathbf{k}})|\gamma_{mi}(\mathbf{k})|^2, \tag{B4}$$

$$E_i = N^{-1}\sum_{m\mathbf{k}}\theta(\epsilon_F-\epsilon_{m\mathbf{k}})|\gamma_{mi}(\mathbf{k})|^2\epsilon_{m\mathbf{k}}. \tag{B5}$$

The k summations are performed numerically by using the tetrahedron method[43] to integrate over the irreducible wedges of the Brillouin zones. For convenience we introduce the following abbreviations:

$$W_{ij} = 2U_{ij} - J_{ij} ,$$

$$m_i = n_i\overline{n}_i ,\ f_{ij} = m_im_j,\ l_i = m_i(\overline{n}_i - n_i) ,$$

$$X_{ij} = (\overline{e}_i - e_i + \overline{e}_j - e_j)f_{ij} ,$$

$$Y_{ijk} = (e_i + e_j - \overline{e}_k)n_in_j\overline{n}_k + (\overline{e}_i + \overline{e}_j - e_k)\overline{n}_i\overline{n}_jn_k .$$

The matrix elements L^{st}_{ijkl}, M^t_{ij} are real and fulfill several symmetry relations. For example $L^{st}_{ijkl} = L^{ts}_{klij}$. Furthermore, one can commute the density or spin operators in A^t_{ij}, which leads to $A^t_{ij} = A^t_{ji}$. Consequently, the symmetry relations $L^{st}_{ijkl} = L^{st}_{ijlk} = L^{st}_{jikl} = L^{st}_{jilk}$ are valid. In the following we list only one representative of each equivalence class and leave out all vanishing matrix elements. Different labels i,j,l denote different orbitals, i.e., $i\neq j, i\neq l, j\neq l$. From Ref. 22 we obtain

$$M^1_{ii} = 2U_{ii}f_{ii}, \tag{B6}$$

$$M^1_{ij} = 2W_{ij}f_{ij}, \tag{B7}$$

$$M^2_{ij} = -\tfrac{3}{2}J_{ij}f_{ij}, \tag{B8}$$

$$L^{11}_{iiii} = 4X_{ii} + 4U_{ii}l_i^2, \tag{B9}$$

$$L^{11}_{iiij} = 4W_{ij}m_if_{ij}, \tag{B10}$$

$$L^{12}_{iiij} = 3J_{ij}m_if_{ij}, \tag{B11}$$

$$L^{11}_{ijij} = 4X_{ij} + 4f_{ij}(U_{ii}m_i+U_{jj}m_j) + 2W_{ij}l_il_j, \tag{B12}$$

$$L^{11}_{ijil} = 4W_{jl}m_if_{jl}, \tag{B13}$$

$$L^{12}_{ijij} = -\tfrac{3}{2}J_{ij}l_il_j, \tag{B14}$$

$$L^{22}_{ijij} = \tfrac{3}{4}X_{ij} + \tfrac{3}{8}(2U_{ij}+J_{ij})l_il_j + \tfrac{3}{2}J_{ij}f_{ij}(n_i\overline{n}_j+\overline{n}_in_j) - \tfrac{3}{4}f_{ij}(U_{ii}m_i+U_{jj}m_j), \tag{B15}$$

$$L^{22}_{ijil} = -\tfrac{3}{4}J_{jl}m_if_{jl}. \tag{B16}$$

APPENDIX C: EXCITED STATES

The one-particle excitations of the system are determined from the retarded Green's functions of the d electrons in band $m=1,\ldots,5$:

$$G^{00}(m,\mathbf{k},t) = -i\theta(t)\langle\Psi_0|[d_{m\mathbf{k}\uparrow}(t), d^\dagger_{m\mathbf{k}\uparrow}(0)]_+|\Psi_0\rangle. \tag{C1}$$

These functions depend upon the susceptibility and frequency matrix elements

$$X^{st}_{ijkl}(m,\mathbf{k}) = (\Omega|\,[B^{s\dagger}_{ij}(m,\mathbf{k}), B^t_{kl}(m,\mathbf{k})]_+\,\Omega), \tag{C2}$$

$$F^{st}_{ijkl}(m,\mathbf{k}) = (\Omega|\,[B^{s\dagger}_{ij}(m,\mathbf{k}), \mathcal{L}B^t_{kl}(m,\mathbf{k})]_+\,\Omega), \tag{C3}$$

where $s,t=0,\ldots,3$ refer to the type of operator [see

Eq. (24)] and $i,j,k,l = 1,\ldots 5$ are the the indices of the atomic d orbitals. They are simply related to the local susceptibility and frequency matrix elements evaluated at a fixed site I:

$$X^{00}(m,\mathbf{k}) = 1, \tag{C4}$$

$$X^{s0}_{ij}(m,\mathbf{k}) = \gamma_{mi}(\mathbf{k}) X^{s0}_{iji}, \tag{C5}$$

$$X^{st}_{ijil}(m,\mathbf{k}) = X^{st}_{ijil}, \tag{C6}$$

$$F^{00}(m,\mathbf{k}) = \epsilon_{m\mathbf{k}} + \frac{1}{4}\sum_i |\gamma_{mi}(\mathbf{k})|^2 W_{ii} X^{01}_{iii} + \frac{1}{2}\sum_{i\neq j} |\gamma_{mi}(\mathbf{k})|^2 W_{ij} X^{01}_{iij}, \tag{C7}$$

$$F^{s0}_{ij}(m,\mathbf{k}) = \gamma_{mi}(\mathbf{k})\Big\{ \epsilon_{m\mathbf{k}} X^{s0}_{iji} + \tfrac{1}{4} W_{ii} X^{s1}_{ijii} + \frac{1}{2}\sum_{k\neq i} [W_{ik} X^{s1}_{ijik} - 4J_{ik}(X^{s2}_{ijik} + X^{s3}_{ijik})] \Big\}, \tag{C8}$$

$$F^{st}_{ijij}(m,\mathbf{k}) = F^{st}_{ijij}. \tag{C9}$$

We list only nonvanishing local matrix elements. As in the case of the ground state, different labels i,j,l imply different orbitals ($i \neq j$, $j \neq l$, $i \neq l$). For simplicity we set $\eta^t_{ij} = \eta^t_{ji}$ in case of $i < j$, $t = 1,2$.

$$X^{11}_{iiii} = 4m_i, \tag{C10}$$

$$X^{11}_{ijii} = -8 f_{ij}\eta^1_{ij}, \tag{C11}$$

$$X^{11}_{ijij} = 2m_j - 8 f_{jj}\eta^1_{jj}, \tag{C12}$$

$$X^{11}_{ijil} = -8 f_{jl}\eta^1_{jl}, \tag{C13}$$

$$X^{12}_{iiij} = \tfrac{3}{4} f_{ij}\eta^2_{ij}, \tag{C14}$$

$$X^{22}_{ijij} = \tfrac{3}{8} m_j - \tfrac{1}{2} f_{jj}\eta^1_{jj} + \tfrac{3}{4} f_{ij}\eta^2_{ij}, \tag{C15}$$

$$X^{22}_{ijil} = -\tfrac{3}{8} f_{jl}\eta^2_{jl}, \tag{C16}$$

$$X^{33}_{ijij} = \tfrac{1}{4}(n_i\overline{n}^2_j + \overline{n}_i n^2_j) - m_j(\eta^1_{jj} m_j - \eta^1_{ij} m_i), \tag{C17}$$

$$X^{01}_{iii} = 8 l_i (\eta^1_{ii})^2 + \sum_{j\neq i} f_{ij}(\overline{n}_i - n_i)[4(\eta^1_{ij})^2 + \tfrac{3}{4}(\eta^2_{ij})^2], \tag{C18}$$

$$X^{01}_{iij} = 8 l_j (\eta^1_{jj})^2 + \sum_{l\neq j} f_{jl}(\overline{n}_j - n_j)[4(\eta^1_{jl})^2 + \tfrac{3}{4}(\eta^2_{jl})^2], \tag{C19}$$

$$F^{11}_{iiii} = 4Y_{iii} + 2W_{ii} l_i, \tag{C20}$$

$$F^{11}_{ijij} = 2Y_{ijj} + W_{ij} l_j, \tag{C21}$$

$$F^{21}_{ijij} = -\tfrac{1}{2} J_{ij} l_j, \tag{C22}$$

$$F^{22}_{ijij} = \tfrac{3}{8} Y_{ijj} + \tfrac{3}{16} W_{ij} l_j + \tfrac{3}{8} J_{ij}(\overline{n}_i - n_i) m_j, \tag{C23}$$

$$F^{13}_{iiij} = J_{ij} m_i (n_j - \overline{n}_j), \tag{C24}$$

$$F^{13}_{ijij} = J_{ij} m_j (n_i \overline{n}_j - \overline{n}_i n_j), \tag{C25}$$

$$F^{33}_{ijij} = \tfrac{1}{4} Y_{jji} + \tfrac{1}{8} W_{jj}(\overline{n}_j - n_j)(n_i\overline{n}^2_j + \overline{n}_i n^2_j) \tag{C26}$$

$$+ \tfrac{1}{4} W_{ij}[\overline{n}^2_i n^2_j - n^2_i \overline{n}^2_j + m_j(n_i\overline{n}_j - \overline{n}_i n_j)], \tag{C27}$$

$$F^{33}_{ijil} = \tfrac{1}{4} J_{jl}(\overline{n}_l - n_l)(n_i\overline{n}^2_j + \overline{n}_i n^2_j). \tag{C28}$$

From these matrix elements $\underline{F}$ and $\underline{X}$ can be calculated, which determine the Green's function matrix $\underline{G}$ in Eq. (20).

[1] D. E. Eastman, F. J. Himpsel, and J. A. Knapp, Phys. Rev. Lett. **40**, 1514 (1978); **44**, 95 (1980); Phys. Rev. B **19**, 2919 (1979).

[2] W. Eberhardt and E. W. Plummer, Phys. Rev. B **21**, 3245 (1980).

[3] H. Mårtensson and P. Nilsson, Phys. Rev. B **30**, 3047 (1984).

[4] S. Hüfner and G. K. Wertheim, Phys. Lett. **47A**, 349 (1974).

[5] C. Guillot, Y. Ballu, J. Paigne, J. Lecante, K. P. Jain, P. Thiry, R. Pinchaux, Y. Petroff, and L. M. Falicov, Phys. Rev. Lett. **39**, 1632 (1977).

[6] F. Aryasetiawan, Phys. Rev. B **46**, 13 051 (1992).

[7] J. Hubbard, Proc. R. Soc. London Ser. A **276**, 238 (1963); **277**, 237 (1964); **281**, 401 (1964).

[8] G. Treglia, F. Ducastelle, and D. Spanjaard, J. Phys. (Paris) **41**, 281 (1980); **43**, 341 (1982).

[9] J. Kanamori, Prog. Theor. Phys. **30**, 275 (1963).

[10] D. R. Penn, Phys. Rev. Lett. **42**, 921 (1979).

[11] A. Liebsch, Phys. Rev. Lett. **43**, 1431 (1979).

[12] A. Liebsch, Phys. Rev. B **23** 5203 (1981).

[13] J. Igarashi, J. Phys. Soc. Jpn. **52**, 2827 (1983); **54**, 260 (1985).

[14] J. Igarashi, in *Core-Level Spectroscopy in Condensed Systems*, edited by J. Kanamori, Springer Series on Solid-State Sciences Vol. 81 (Springer Berlin, 1988).

[15] L. M. Roth, Phys. Rev. **186**, B428 (1969).

[16] J. A. Hertz and D. M. Edwards, J. Phys. **3**, 2174 (1973); **3**, 2191 (1973).

[17] H. Matsumoto, L. Umezawa, S. Seki, and M. Tachiki, Phys. Rev. B **17**, 2276 (1978).

[18] L. C. Davis and L. A. Feldkamp, Solid State Commun. **34**, 141 (1980).

[19] R. H. Victora and L. M. Falicov, Phys. Rev. Lett. **55**, 1140 (1985); Phys. Rev. B **30**, 1695 (1984).

[20] T. Jo and G. A. Sawatzky, Phys. Rev. B **43**, 8771 (1991); A. Tanaka, T. Jo, and G. A. Sawatzky, J. Phys. Soc. Jpn. **61**, 2636 (1992); A. Tanaka and T. Jo, *ibid.* **62**, 2636 (1993).

[21] G. Stollhoff and P. Thalmeier, Z. Phys. B **43**, 13 (1981).

[22] A. M. Oleś and G. Stollhoff, Phys. Rev. B **29**, 314 (1984).

[23] M. Takahashi and J. Kanamori, in *Interatomic Potential and Structural Stability*, edited by K. Tarakura and H. Akai, Springer Series in Solid State Sciences Vol. 114 (Springer, Berlin, 1993).

[24] S. Horsch, P. Horsch, and P. Fulde, Phys. Rev. B **28**, 5977 (1983); **29**, 1870 (1984).

[25] W. Borrmann and P. Fulde, Phys. Rev. B **35**, 9569 (1987).

[26] K. W. Becker, W. Brenig, and P. Fulde, Z. Phys. B **81**, 165 (1990).

[27] H. Mori, Prog. Theor. Phys. **34**, 423 (1965).

[28] R. Zwanzig, *Lectures in Theoretical Physics* (Interscience, New York, 1961), Vol. 3.

[29] O. K. Andersen, Phys. Rev. B **12**, 3060 (1975).

[30] P. Thalmeier and L. M. Falicov, Phys. Rev. B **20**, 4637 (1979).

[31] M. Tinkham, *Group Theory and Quantum Mechanics*

(McGraw-Hill, New York, 1964).
[32]K. W. Becker and P. Fulde, Z. Phys. B **72**, 423 (1988); J. Chem. Phys. **91**, 4223 (1989).
[33]R. Kubo, J. Phys. Soc. Jpn. **17**, 1100 (1962).
[34]J. Goldstone, Proc. R. Soc. London Ser. A **239**, 267 (1957).
[35]T. Schork and P. Fulde, J. Chem. Phys. **97**, 9195 (1992).
[36]P. Fulde, *Electron Correlations in Molecules and Solids*, Springer Series in Solid-State Sciences Vol. 100 (Springer, Berlin, 1991).
[37]F. Kayzar and J. Friedel, J. Phys. (Paris) **39**, 379 (1978).
[38]W. Metzner and D. Vollhardt, Phys. Rev. Lett. **62**, 325 (1989).
[39]K. W. Becker and W. Brenig, Z. Phys. B **79**, 195 (1990).
[40]F. Forster, *Hydrodynamic Fluctuations, Broken Symmetry and Correlation Functions* (Benjamin, New York, 1975).
[41]L. M. Roth, Phys. Rev. **184**, B451 (1969).
[42]J. Igarashi, P. Unger, K. Hirai, and P. Fulde, Phys. Rev. B **49**, 16 181 (1994).
[43]G. Lehmann, P. Rennert, M. Taut, and H. Wonn, Phys. Status Solidi **37**, K27 (1970); G. Lehmann and M. Taut, Phys. Status Solidi B **54**, 469 (1972).
[44]O. K. Andersen and O. Jepsen, Physica B **91**, 317 (1977).
[45]D. van der Marel and G. A. Sawatzky, Phys. Rev. B **37**, 10 674 (1988).
[46]C. S. Wang and J. Callaway, Phys. Rev. B **15**, 298 (1977).
[47]V. L. Moruzzi, J. F. Janak, and A. R. Williams, *Calculated Electronic Properties of Metals* (Pergamon, New York, 1978).
[48]T. Aisaka, T. Kato, and E. Haga, Phys. Rev. B **28**, 1113 (1983).